Trans Indian Inst Met (2017) 70(2):497–509
DOI 10.1007/s12666-016-1009-2

TECHNICAL PAPER

Studies on the Bioremediation of Chromium from Aqueous Solutions Using *C. paurometabolum*

Divyasree C. Prabhakaran[1] · S. Subramanian[1]

Received: 5 October 2016 / Accepted: 15 November 2016 / Published online: 22 November 2016

Abstract The potential of *Corynebacterium paurometabolum*, a Gram positive acid fast bacterium, has been investigated as a biosorbent for the remediation of Cr(VI) and Cr(III). A complete bioremediation of Cr(VI) has been achieved at an equilibrium time of 2 h, initial Cr(VI) concentration of 4 mg/L, pH 1 and a biomass loading of 3.1×10^{10} cells/mL, with equal contributions from biosorption and bioreduction processes, while 55% biosorption has been accomplished at an equilibrium time of 2 h, initial Cr(III) concentration of 4 mg/L, pH 3 and a biomass loading of 3.4×10^{10} cells/mL with respect to the bioremediation of Cr(III). The biosorption isotherms of Cr(VI) and Cr(III) exhibited a typical Langmuirian behaviour. The Gibbs free energies (ΔG) have been determined to be -25.5 and -29.5 kJ/mol respectively for Cr(VI) and Cr(III), suggestive of chemisorption. The desorption studies have indicated only a marginal release of Cr(VI)/Cr(III) into the bulk solution, attesting to the irreversible nature of biosorption. FTIR studies have revealed the involvement of hydroxyl, carboxyl, amino and phosphate groups in the biosorption of Cr(VI)/Cr(III). Electrokinetic and X-ray photoelectron spectroscopic studies have provided evidence in support of the biosorption and bioreduction mechanisms of chromium remediation.

Keywords Cr(VI) · Cr(III) · *C. paurometabolum* · Biosorption · Bioreduction · Langmuir model

1 Introduction

Water pollution mainly caused by heavy metal such as chromium poses a major threat to the living beings as a result of anthropogenic activities that includes mining, production of steel, leather tanning, chrome plating, paint and dye manufacturing etc. Hexavalent chromium (Cr(VI)) is recognised as a potent carcinogen by the World Health Organisation (WHO), the International Agency for Research on Cancer and the Environmental Protection Agency (EPA) in USA [1–3]. However, trivalent chromium (Cr(III)) is considered less toxic and it is an important micronutrient essential for mammalian metabolism, maintaining blood glucose and cholesterol levels [4–6].

The conventional methods available for chromium pollution mitigation such as chemical precipitation, membrane filtration, ion exchange and electrochemical separation have certain drawbacks such as high operational cost and more importantly secondary pollution in the form of sludge [7–10]. Thus it becomes pertinent to opt for a more promising and ecofriendly alternative, the bioremediation process [11]. Biosorption is a bioremediation process that is defined as a physico-chemical process which involves the binding/concentrating of contaminant ions from aqueous solution by a biological material/biomass [12–15]. There are various biosorbents being used such as bacteria, fungi, algae, plants and also industrial and agricultural waste biomass that includes, activated sludge, fermentation wastes etc. [16–18]. Among them, bacterial cells as biosorbents are gaining recognition because of their

Electronic supplementary material The online version of this article (doi:10.1007/s12666-016-1009-2) contains supplementary material, which is available to authorized users.

✉ S. Subramanian
ssmani@materials.iisc.ernet.in

[1] Department of Materials Engineering, Indian Institute of Science, Bangalore, Karnataka 560012, India

ubiquity, ability to grow under controlled conditions and small size, which leads to high surface area and hence faster rates of pollution remediation [14, 17, 19].

Chromium bioremediation has been investigated using bacterial strains belonging to genus such as *Bacillus*, *Enterobacter*, *Escherichia*, *Microbacterium*, *Zoogloea*, *Agrobacterium*, *Aeromonas*, *Ochrobactrum*, *Acinetobacter*, *Arthrobacter*, *Staphylococcus and Pseudomonas* [18–23]. The present work investigates the capability of *C. paurometabolum* in the bioremediation of Cr(VI) and Cr(III) ions and the mechanisms involved in the process is deduced from the results obtained by adopting different characterisation techniques.

2 Materials and Methods

2.1 Analytical Reagents

Analytical grade $K_2Cr_2O_7$ and $CrCl_3{\cdot}6H_2O$, sources for Cr(VI) and Cr(III) respectively, were purchased from Merck, Germany and Loba Chemie, India. NaOH and HCl used for the pH adjustment were also of analytical grade. Analytical grade 1,5 diphenylcarbazide, a Cr(VI) complexing agent was obtained from Merck, Germany for UV–Vis spectrophotometric analysis. Other reagents used for the experiments such as, H_2SO_4 and acetone were all of analytical grade. Deionised water of resistivity 18.2 MΩ cm from a MilliQ system was used in all the experiments.

2.2 Microorganism and Growth Conditions

A pure strain of *Corynebacterium paurometabolum* (MTCC No. 6841) was procured from the Institute of Microbial Technology (IMTECH), Chandigarh, India and cultured using Nutrient broth medium (NB) of pH 7, the constituents of which are 5 g/L peptone, 2 g/L yeast extract, 1 g/L beef extract and 5 g/L NaCl. The medium containing 10% of the freshly inoculated bacteria was agitated in an Orbitek orbital shaker at a temperature of 30 °C for 24 h. The growth was analysed by cell enumeration using a Petroff-Hausser counter in conjunction with a Leitz phase contrast microbiological microscope (Laborlux K Wild MPS 12).

2.3 Estimation of Chromium

The total chromium in the samples was estimated using a Thermo Electron Corporation M Series Atomic Absorption Spectrometer (AAS). The concentration of Cr(VI) in the solution was estimated by 1,5 diphenylcarbazide (DPC) method using a Labomed Inc. UV–Vis spectrophotometer at the wavelength of 540 nm. The concentration of Cr(III) present in the sample was computed by subtracting Cr(VI) concentration obtained using DPC method from the total Cr concentration obtained using AAS.

2.4 Biomass Preparation

For the biosorption experiments, an appropriate volume of *C. paurometabolum* bacterial culture grown in NB medium for 24 h was centrifuged at 10,000 rpm for 10 min using a Remi refrigerated centrifuge. Subsequently, the obtained pellet was washed thoroughly with deionised water and used for the experiments. The bacterial cells were enumerated using a Petroff-Hausser cell counting chamber.

2.5 Biosorption Test Procedure

A known amount of the bacterial pellet of desired cell count was dispersed in chromium solution of desired concentration and the pH adjusted to a chosen value using a Systronics digital pH meter. The samples were made up to a final volume of 100 mL in 250 mL Erlenmeyer flasks and were then agitated in a Orbitek rotary shaker at 30 °C for a desired period of time. The suspensions were then centrifuged in a Remi refrigerated centrifuge at 10,000 rpm for 10 min. The chromium concentration in the supernatant was determined and the amount biosorbed by the bacterial cells was estimated by difference. The pH values of the solutions were also monitored after the adsorption process and hardly any change (<0.1 unit) was observed in the chosen range and hence the initial pH values have been reported.

2.6 Desorption Studies

For the desorption studies, chromium interacted bacterial cells obtained after the biosorption experiment were centrifuged at 10,000 rpm for 10 min to obtain a pellet which was then redispersed in deionised water adjusted to the respective pH that was used for the corresponding biosorption experiments. As described earlier, HCl and NaOH were used for adjusting the pH values. These samples were then agitated in an orbital shaker at 30 °C for 2 h. The Cr(VI) and total chromium concentration for the biosorption/desorption experiments were determined as per the procedures mentioned earlier.

2.7 Attenuated Total Reflectance-Fourier Transform Infrared (ATR-FTIR) Spectroscopy

The biomass samples both before and after interaction with chromium ions were freeze dried for 12 h and the samples were loaded onto to the diamond crystal of the Bruker

ALPHA FTIR spectrophotometer and the spectra were recorded in the mid-IR wavenumber range of 4000–400 cm^{-1}.

2.8 X-ray Photoelectron Spectroscopy (XPS)

XPS analysis was carried out using Kratos Axis DLD X-ray Photoelectron Spectrometer with monochromatic Al Kα (hυ = 1486.61 eV) X-ray radiation. For the analysis, the freeze dried bacterial samples before and after interaction with chromium ions were pressed into pellets in order to obtain a thin disc. The high resolution spectra for the elements such as chromium, carbon, oxygen, nitrogen, phosphorus and sulphur were recorded using a 20 eV pass energy. Pass energy, is the energy to which the photoelectrons decelerate to, after retardation of the electric field by the electron optical system. This enables a high resolution spectrum to be obtained. The calibration of the binding energies of elements was performed with C(1 s) peak of the aliphatic carbon, which is at 284.6 eV.

2.9 Electrokinetic Studies

The zeta potential of the bacterial cells both before and after Cr biosorption experiments were recorded using Zetasizer Nanoseries (Nano-ZS90) manufactured by Malvern Instruments Ltd. Worcestershire, UK. These studies were carried out as a function of pH in the range of 1–12. The equilibrium time and cell concentration were maintained as 2 h and 2×10^9 cells/mL respectively. 10^{-3} M NaCl solution was used as the indifferent electrolyte. The effect of Cr(VI) concentration on the zeta potential was investigated in the range of 4–400 mg/L. Zeta potential studies were also carried out for the bacterial cells subsequent to the interaction with different concentrations of Cr(III), namely 4, 40 and 400 mg/L. Following the zeta potential measurements, the residual concentrations of Cr(VI) and Cr(III) were also determined as a function of pH, in the absence and presence of bacterial cells.

All the above experiments were carried out in duplicate and the standard deviation was determined.

3 Results and Discussion

3.1 Bioremediation Studies of Chromium Using *C. paurometabolum*

3.1.1 Growth Studies

The growth curve for *C. paurometabolum* is portrayed in Fig. 1. From the growth curve, it can be observed that the lag phase is absent since active bacterial cultures were used. It is evident from the growth curve obtained that the bacterial count increases exponentially up to 8 h from 1.28×10^8 cells/mL to 8×10^9 cells/mL after which the stationary phase is attained (Fig. 1). The bacterial cells from the stationary phase (∼24 h) were harvested for the subsequent bioremediation studies. The generation time calculated from the growth curve is found to be 1.6 h/gen.

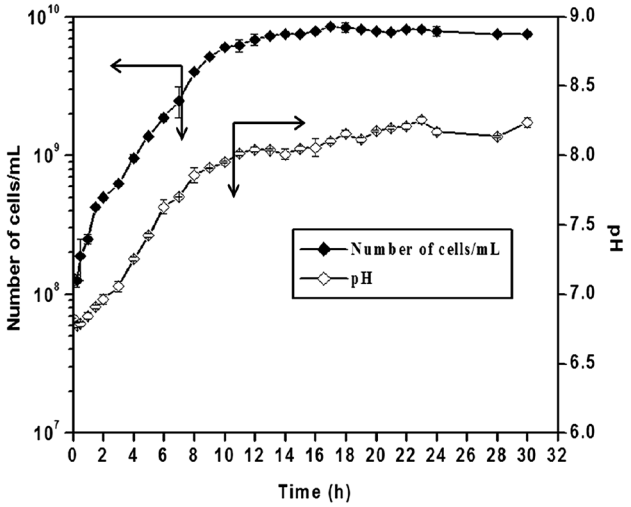

Fig. 1 Growth curve of *C. paurometabolum* bacterial cells with change in pH with growth

Simultaneously, the change in pH over the period of bacterial growth was also monitored during the growth analysis. The pH of the medium is found to increase from 6.8 to about 8.2 during the growth of *C. paurometabolum* bacterial cells (Fig. 1). This can be attributed to the deamination reaction occurring as a result of metabolic activity of the bacteria during its growth period.

3.1.2 Biosorption Kinetics

The effect of contact time on the biosorption of the chromium ions with *C. paurometabolum* bacterial cells was initially studied. For this, 2.6×10^9 cells/mL (corresponding to 15 mg dry weight of the bacterial cells) were interacted with Cr(VI) and Cr(III) solutions each of concentration 4 mg/L each at pH 2 for varying time intervals at 30 °C. From Fig. 2a, it is clear that total chromium biosorption increases with increase in contact time up to 1.2 h after which a plateau is attained. About 12% total Cr biosorption is achieved during this time period. In the further biosorption experiments, an equilibrium time of 2 h was maintained. Based on the estimations of total Cr and Cr(VI), it is interesting to observe that, bioreduction of Cr(VI) to Cr(III) occurs in concurrence with the biosorption process. The percentage of bioreduction process is found to increase with increase in contact time of the Cr(VI) ions with the bacterial cells (Fig. 2a). In the case of

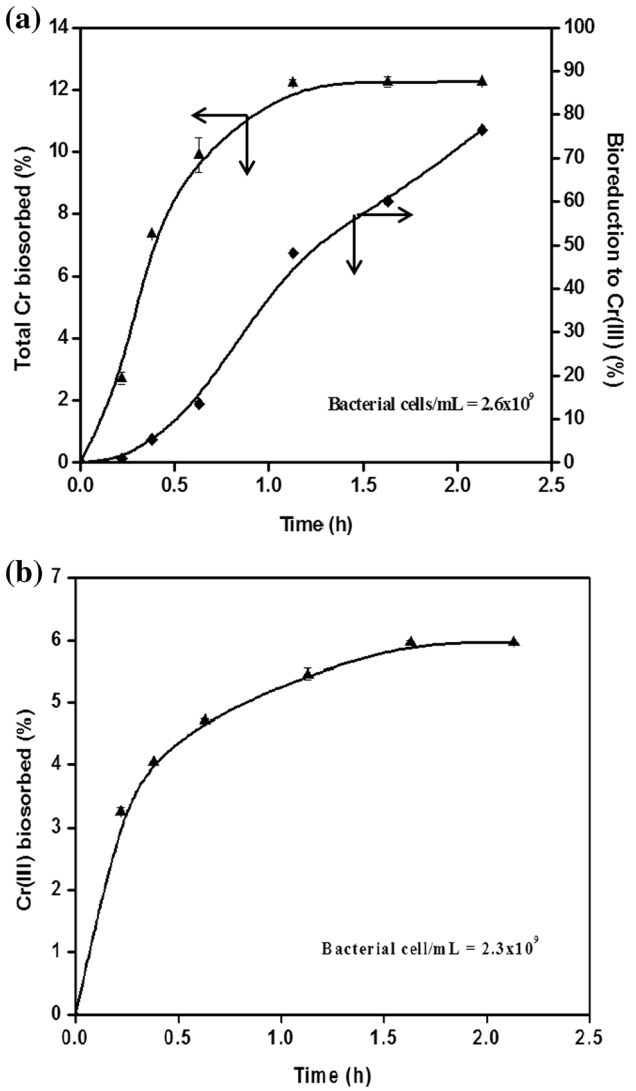

Fig. 2 Effect of contact time on **a** Cr(VI) and **b** Cr(III) biosorption using *C. paurometabolum* bacterial cells [Cr(VI)/Cr(III) = 4 mg/L, pH 2 and 30 °C]

Cr(III) biosorption using *C. paurometabolum* bacterial cells, the kinetics of Cr(III) biosorption is depicted in Fig. 2b, which shows a similar trend as that observed for Cr(VI). The biosorption of Cr(III) increases with time up to about 1.5 h and subsequently attains saturation. In subsequent experiments with Cr(III), the equilibrium time was fixed at 2 h.

The biosorption kinetics data presented in Fig. 2a, b were fitted to various kinetic models to evaluate the kinetics of Cr(VI) and Cr(III) biosorption by *C. paurometabolum* using the linearised forms of the pseudo first order and pseudo second order kinetic expressions represented in Eqs. (1) and (2) respectively, as given below:

$$\log(q_e - q_t) = -k_1 t/2.303 + \log(q_e) \quad (1)$$

$$t/q_t = 1/(k_2 q_e^2) + t/q_e \quad (2)$$

where, q_e is the Cr biosorbed at equilibrium per gram of cells, q_t is Cr biosorbed at any time t, k_1 and k_2 are the velocity constants for pseudo first order and pseudo second order respectively [18].

The Cr(VI) biosorption kinetics using the bacterial cells is found to follow pseudo first order kinetics ($R^2 = 0.98$) with the velocity constant (k_1) obtained as 0.09 min^{-1} (Supplementary Figure S1(a)). On the other hand, Cr(III) biosorption is found to follow pseudo second order kinetics ($R^2 = 0.99$) with the velocity constant (k_2) obtained as 0.04 gmg^{-1} min^{-1} (Supplementary Figure S1(b)).

3.1.3 Effect of pH on Biosorption

The solution pH is an important factor that affects the biosorption process. In order to find out the effect of pH on the biosorption studies, the pelleted fully grown bacterial cells of count 2.6 × 10^9 cells/mL (corresponding to 15 mg dry weight of the bacterial cells) were dispersed in Cr(VI) and Cr(III) solutions of concentration 4 mg/L each at varying pH from 1 to 6 and allowed to equilibrate for 2 h. From Fig. 3a it is evident that in the absence of bacterial cells, Cr(VI) is stable over the pH range chosen for the study. The percentage of total Cr biosorbed is found to decrease from 13% to about 7% as the pH is increased from 1 to 6, due to the electrostatic repulsion of negatively charged oxyanion of Cr(VI) with the negatively charged functional groups present on the bacterial cell surface as shown in Fig. 3a. From pH 1–6 Cr(VI) exist as $HCrO_4^-$ oxyanions in aqueous solutions [24–26]. The bacterial cell surface at very low (acidic) pH becomes protonated and attain a positive charge, facilitating the biosorption of Cr(VI) to a greater extent. Figure 3a also shows that the bioreduction of Cr(VI) to Cr(III) is maximum at pH 1 (81%) and decreases sharply to about 11% at pH 4. The bioreduction is below 5% between pH 5 and 6. The biosorption study of Cr(III) using the bacterial cells as a function of pH is depicted in Fig. 3b. In the absence of the bacterial cells, it is evident that Cr(III) is stable up to pH 3 and thereafter its concentration decreases in solution due to precipitation. As per the Pourbaix (Eh–pH) diagram for the Cr(III)-H_2O system, it can be observed that Cr(III) exists as positively charged species such as Cr^{3+} in the pH range of 1–4. Positively charged hydroxo species such as $Cr(OH)^{2+}$ and $Cr(OH)_2^+$ also exist in the pH range of 3.8–6.3. However, in the pH range of 5.5–12, Cr(III) starts precipitating as trihydroxochromium ($Cr(OH)_3$ [24–26]. On the other hand, in the presence of the bacterial cells, the Cr(III) concentration continuously decreases from 4 mg/L at pH 1 to about 0.93 mg/L at pH 6, predominantly by biosorption and partially by precipitation processes (Fig. 3b).

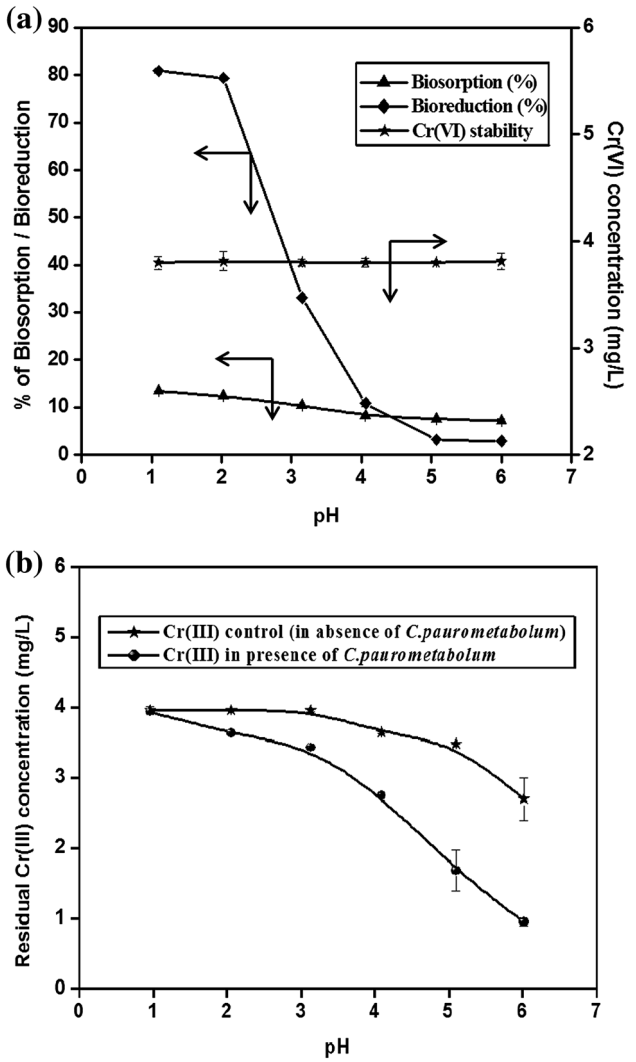

Fig. 3 Effect of pH on Cr biosorption [Cr(VI)/Cr(III) = 4 mg/L, equilibrium time (t_e) = 2 h, 2.6 × 10^9 cells/mL and 30 °C]: **a** Cr(VI) stability and % biosorption and bioreduction using *C. paurometabolum*; **b** Cr(III) stability and uptake in the presence of *C. paurometabolum* bacterial cells

Therefore, taking into consideration the bioremediation of Cr(III) only by biosorption, pH 3 was chosen for the further studies, at which pH, Cr(III) exists as only positively charged Cr^{3+} ions.

3.1.4 Effect of Biomass Loading

The effect of biomass loading on Cr biosorption was studied by varying *C. paurometabolum* cell concentration from 2.3 × 10^9 to 4.6 × 10^{10} cells/mL (corresponding to 13 mg to 300 mg dry weight of the bacterial cells, respectively). The Cr(VI) biosorption experiments were conducted at pH 1 for an equilibration time of 2 h, and the initial Cr(VI) concentration was 4 mg/L. Figure 4a shows that the percentage biosorption increases with increase in cell concentration, which is attributable to the increase in surface binding sites. A maximum biosorption of 50.3% biosorption is obtained for a biomass loading of 3.1 × 10^{10} cells/mL (corresponding to 180 mg dry weight of the bacterial cells), and this was fixed as the optimum biomass concentration for further studies. It can also be noted from Fig. 4a that the specific uptake of Cr(VI) is found to decrease with increase in biomass loading. This arises due to the crowding of cells resulting in the masking of the functional groups exposed per bacterial and the phenomenon is known as 'screen effect' that has also been reported by other researchers [27]. From Fig. 4b, it is evident that the bioreduction process is observed to increase with increase in biomass loading, testifying to the requirement of more electron donor functional groups. At a higher biomass loading, it is also observed that a complete bioreduction of Cr(VI) to Cr(III) occurs with a nil concentration of Cr(VI) (Fig. 4b). Thus a complete remediation of Cr(VI) ions could be achieved, adhering to the USEPA regulations. A concurrent increase in the Cr(III) concentration in solution can also be observed in Fig. 4b. Biosorption experiments of Cr(III) carried out using *C. paurometabolum* bacterial cells conducted at pH 3 resulted in a maximum biosorption of 55% of Cr(III) at a biomass loading of 3.4 × 10^{10} cells/mL (corresponding to 200 mg dry weight) as depicted in Fig. 4c. The specific uptake of Cr(III) shows a similar trend to that observed in the case of Cr(VI) as shown in Fig. 4c.

3.1.5 Biosorption–Desorption Isotherm

The biosorption isotherm experiments were carried out by interacting *C. paurometabolum* bacterial cells (3.1 × 10^{10} cells/mL corresponding to 180 mg dry weight and 3.4 × 10^{10} cells/mL corresponding to 200 mg dry weight, respectively) with Cr(VI) and Cr(III) ions respectively. Figure 5a shows the biosorption isotherm of Cr(VI) for *C. paurometabolum* bacterial cells. It is evident from Fig. 5a that the amount biosorbed increases with increase in chromium concentration and subsequently tends to attain saturation coverage beyond 5 mg/L equilibrium chromium concentration. The shape of the isotherm may be categorised as L-type of the Giles classification [28], indicating that it is monolayer adsorption of Cr ions onto the bacterial cell surface. It becomes imperative to ascertain the nature of interaction between the bacterial cells and Cr(VI) ions. Hence, desorption tests were carried on the Cr(VI) biosorbed bacteria by maintaining the same conditions as that optimised for the biosorption process, namely, biomass loading of 3.4 × 10^{10} cells/mL, pH 1 and 30 °C. It is apparent from the desorption isotherm of Cr(VI) that desorption of chromium from the bacterial cell surface could be achieved only to a smaller extent, about 12% Cr, thereby

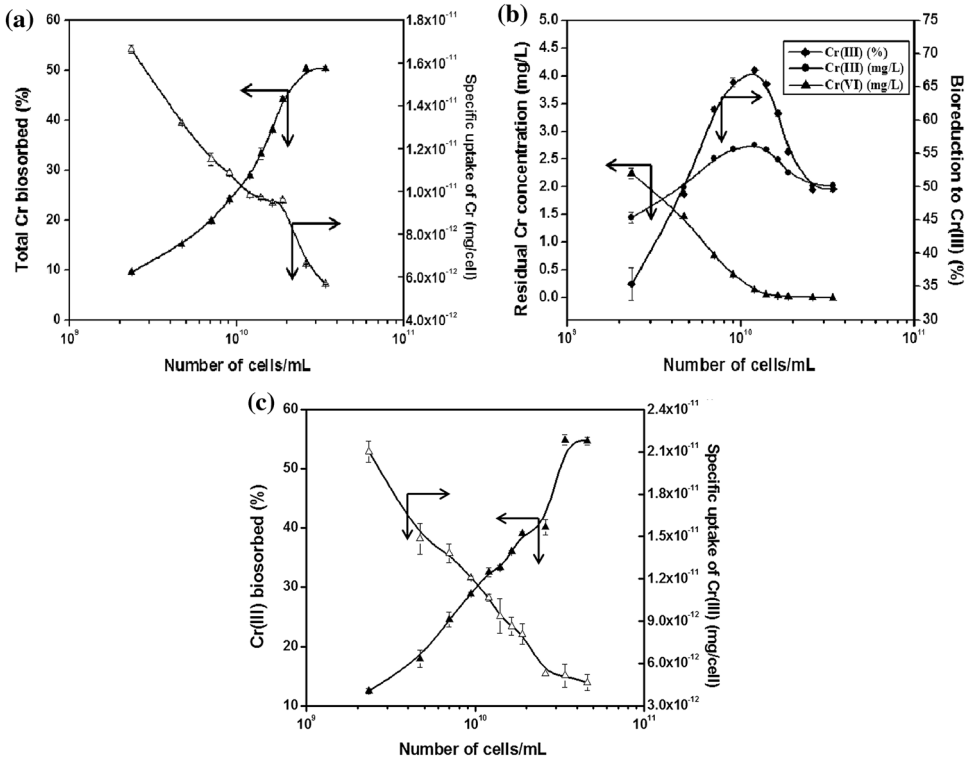

Fig. 4 Effect of biomass loading on Cr biosorption using *C. paurometabolum* [Cr(VI)/Cr(III) = 4 mg/L, t_e = 2 h and 30 °C]: **a** Total Cr biosorption (%) and specific uptake (mg/cell) at pH 1; **b** Residual Cr(VI) and Cr(III) concentration and % bioreduction as a function of concentration of bacterial cells; **c** Cr(III) biosorption (%) and specific uptake (mg/cell) at pH 3

indicating the irreversible nature of the biosorption process due to the chemical forces of binding between Cr(VI) and the bacterial cells (Fig. 5a).

Additionally, a set of independent experiments was carried out to determine the biosorption–desorption characteristics of Cr(III) on the bacterial cells and the results are depicted in Fig. 5b. It can be observed from Fig. 5b that the biosorption isotherm of Cr(III) follows a similar trend to that observed for Cr(VI), namely an initial increase in the biosorption density at lower concentrations followed by attainment of a plateau at higher concentrations. In this case too, the isotherm may be categorized as L-type of the Giles classification [28]. The desorption results shown in Fig. 5b for Cr(III) further attest to the irreversible nature of biosorption, corroborated by the partial desorption of the Cr(III) biosorbed. The maximum desorption that could be achieved is about 30% at a low concentration.

The biosorption isotherms for Cr(VI) and Cr(III) for the bacterial cells *C. paurometabolum* are found to adhere to the Langmuir model [29] (Supplementary Figures S2(a) and S2(b)) with a good correlation ($R^2 \approx 0.99$). The maximum Cr(VI) biosorption capacity of the bacterial cells was estimated as 2.5 mg/g, whereas for Cr(III) biosorption, the value was found to be 1.1 mg/g. The free energy (ΔG) values determined using the Langmuir constants related to energy of biosorption, were found to be −25.5 and −29.5 kJ/mol for Cr(VI) and Cr(III) biosorption respectively. The values for ΔG indicate the involvement of chemical binding forces in the biosorption process [12].

3.2 Elucidation of the Mechanisms Involved in the Bioremediation of Cr(VI)/Cr(III) Ions Using *C. paurometabolum*

3.2.1 ATR-FTIR Spectroscopic Studies

FTIR spectral studies were performed to identify various functional groups present on *C. paurometabolum* and their involvement in the biosorption of Cr(VI) and Cr(III) ions. On comparing the spectra obtained for the bacterial cells before and after biosorption of Cr(VI) as shown in Fig. 6a, b, it can be observed certain apparent shifts in the wavenumber for the identified functional groups. The functional groups were identified with the help of standard wavenumber values [30]. The broad band obtained at 3273 cm^{-1} corresponding to hydroxyl (–OH) and amino (–NH) group stretching in the case of the bacterial cells alone is shifted to 3261 cm^{-1} for Cr(VI) biosorbed bacteria. Similarly, a shift in the amide I band is also observed from 1644 to 1634 cm^{-1}. Apparent shifts in the wavenumber corresponding to the (–CO) stretching of carboxyl group (–COOH) and (P=O) stretching can be observed from 1393 and 1232 to 1380 and 1223 cm^{-1} respectively. In the case of the bacterial cells interacted with Cr(III) ions, apart from similar shifts in

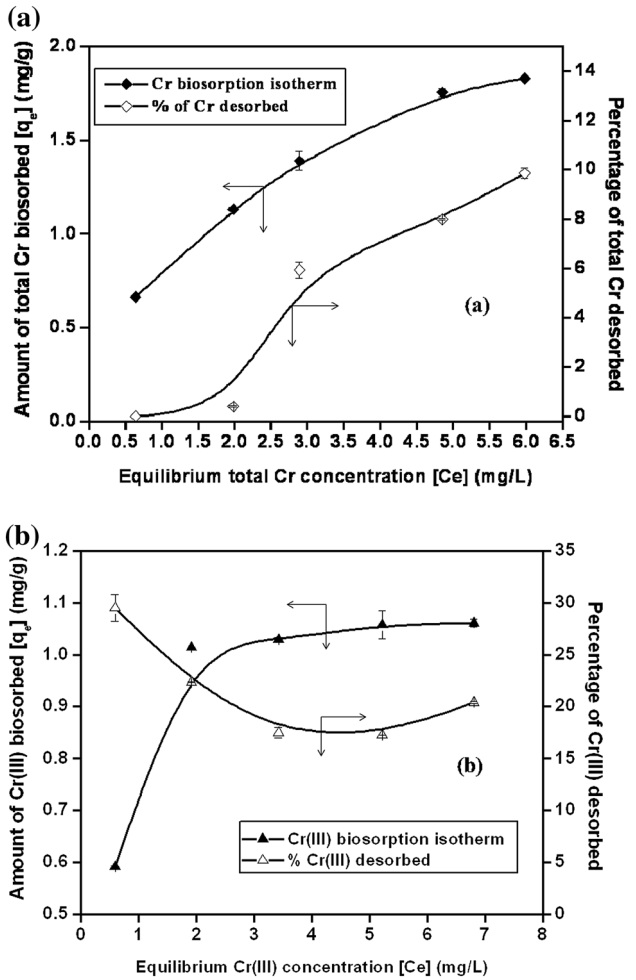

Fig. 5 **a** Cr(VI) biosorption isotherm and percentage of desorption of Cr from *C. paurometabolum*; **b** Cr(III) biosorption isotherm and percentage of desorption of Cr(III) from *C. paurometabolum*

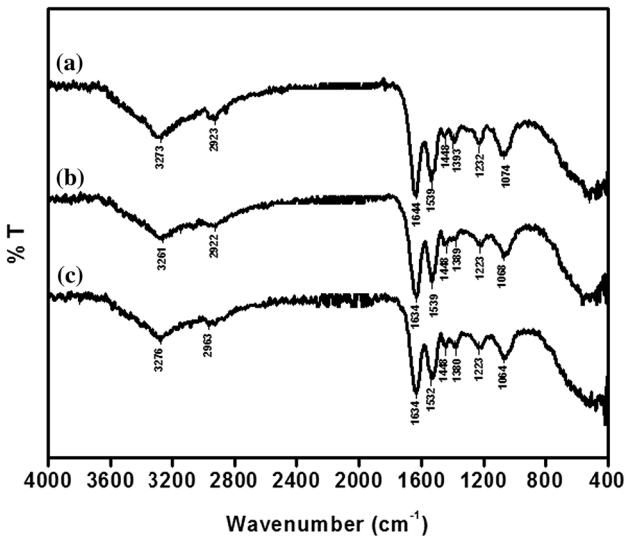

Fig. 6 ATR-FTIR spectra of: *a C. paurometabolum*, *b* Cr(VI) interacted *C. paurometabolum* and *c* Cr(III) interacted *C. paurometabolum*

wavenumbers of functional groups as those obtained for Cr(VI) biosorbed bacteria can be observed. Apart from this, Cr(III) biosorbed bacteria showed a shift in wavenumber to 1532 cm^{-1} corresponding to amide II band from 1539 cm^{-1} observed for the bacteria alone (Fig. 6c). The functional groups observed in the case of *C. paurometabolum* bacterial cells before interaction with chromium are in good agreement with those reported earlier for a Gram positive bacterium [31].

3.2.2 XPS Analysis

In order to ascertain the redox state of chromium bound on the bacterial cell surface consequent to the biosorption process, X-ray photoelectron spectra of *C. paurometabolum* cells before and after interaction with Cr(VI) and Cr(III) were recorded. The high resolution XPS spectrum of Cr(2p) obtained for Cr(VI) interacted bacterial cells as shown in Fig. 7a, indicates the presence of both Cr(VI) and Cr(III) on the cell surface substantiating that the bioreduction process not only results in the presence of Cr(III) in the solution (Fig. 2a) but also gets bound onto the bacterial cell surface. The two doublet peaks obtained with the binding energies of 579.0 and 589.0 eV correspond to $2p_{3/2}$ and $2p_{1/2}$ of Cr(VI), while 576.3 eV and 586.3 eV correspond to $2p_{3/2}$ and $2p_{1/2}$ of Cr(III) for the bacterial cells interacted with Cr(VI) ions. In the case of Cr(2p) spectra recorded for Cr(III) interacted bacterial cells as shown in Fig. 7b, binding energies of 577.7 eV/587.7 eV corresponding to the $2p_{3/2}/2p_{1/2}$ of Cr(III) can be observed. These binding energy values are in close agreement with the values obtained by other workers, Dambies et al. [32] and Park et al. [33].

The role of other functional groups in the bioremediation process was assessed by recording high resolution X-ray photoelectron spectra for C(1s), O(1s), N(1s), P(2p) and S(2p) for the bacterial cells before and after interaction with Cr(VI)/Cr(III) ions (Fig. 7c–g) and the binding energy values are tabulated in Table 1. In the case of the high resolution spectra obtained for C(1s) as depicted in Fig. 7c, a marginal shift in the binding energies for functional groups C–O/C–N/C=O after Cr(VI)/Cr(III) of biosorption can be observed (Table 1). Binding energies shifts can be observed from the high resolution spectra obtained for O(1s) for both the bacterial cells as shown in Fig. 7d for the functional groups such as –O–C/P–O–C/C–O–C after biosorption of Cr vis-à-vis the bacterial cells alone. In the case of other oxygen containing functional groups such as O–H/O=C/O=P, there is not much of a shift in binding energies obtained (Table 1). A shift in binding energies for –NH functional group is also found in N(1s) high

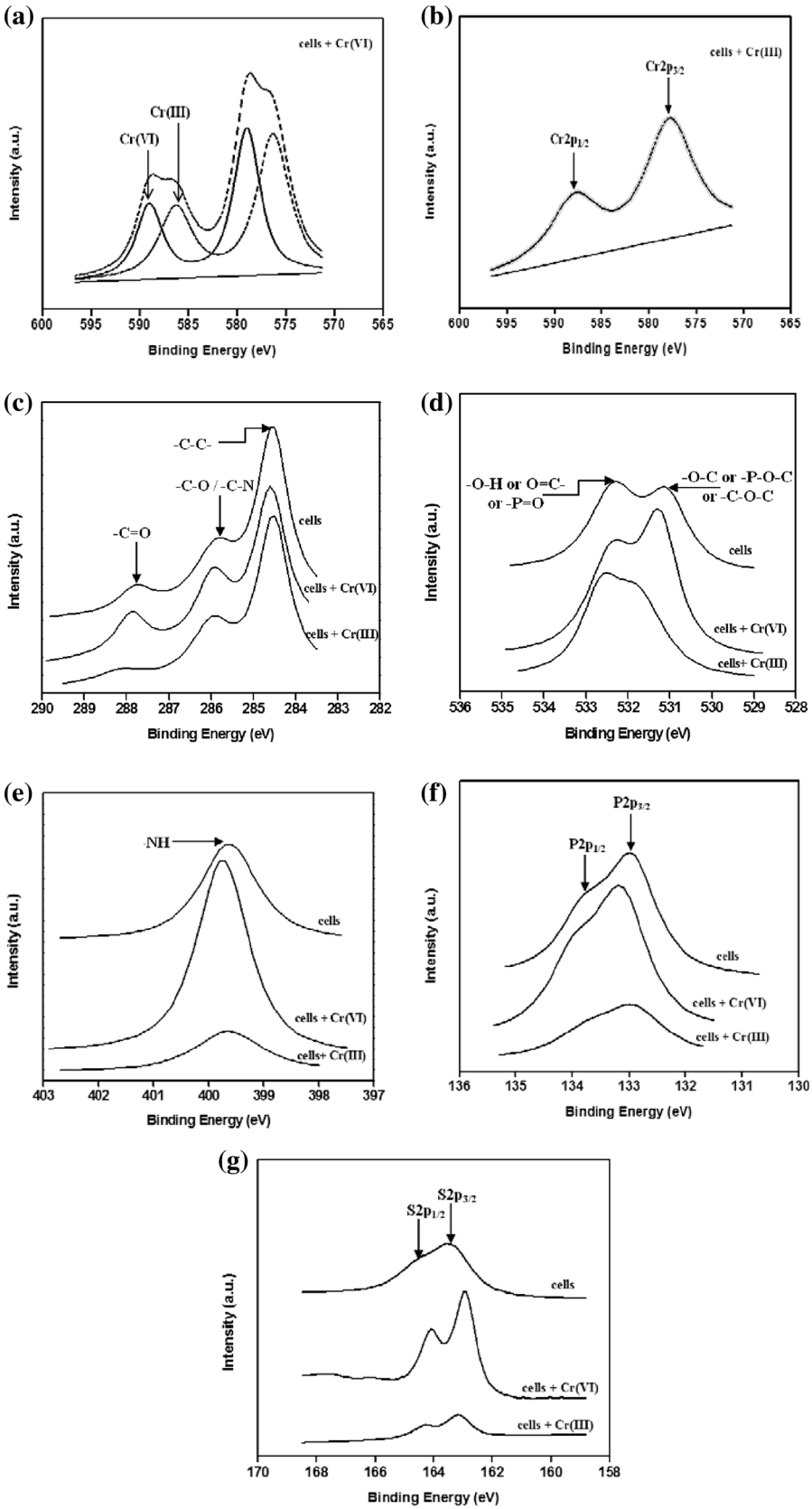

Fig. 7 High resolution X-ray photoelectron spectra of *C. paurometabolum* for: **a** Cr(2p) after interaction with Cr(VI), **b** Cr(2p) after interaction with Cr(III), **c** C(1 s), **d** O(1 s), **e** N(1 s), **f** P(2p) and **g** S(2p)

Table 1 Binding energy (eV) values obtained for elements present in *C. paurometabolum* before and after interaction with Cr(VI) and Cr(III) using XPS

Samples	Elements present in the samples analysed using XPS and their corresponding binding energy (eV)														
	Cr(2p)				C(1s)			O(1s)		N(1s)	P(2p)		S(2p)	
	Cr(VI)		Cr(III)		C–C	C–O or C–N	C=O	O–C or P–O–C or C–O–C	–OH or O=C or P=O	–NH	$2p_{3/2}$	$2p_{1/2}$	$2p_{3/2}$	$2p_{1/2}$
	$2p_{3/2}$	$2p_{1/2}$	$2p_{3/2}$	$2p_{1/2}$										
C. paurometabolum	–		–		284.6	285.8	287.8	531.1	532.3	399.6	133.0	133.8	163.5	164.6
Cr(VI) interacted *C. paurometabolum*	579.0	589.0	576.3	586.3	284.6	531.3	287.9	532.7	532.3	399.8	133.2	134.0	163.0	164.1
Cr(III) interacted *C. paurometabolum*	–		577.7	587.7	284.5	286.0	531.8	532.7	532.5	399.7	133.0	133.8	163.1	164.3

resolution spectra for the bacterial cells consequent to Cr(VI)/Cr(III) biosorption (Fig. 7e). Apparent shifts in binding energies obtained for P(2p) and S(2p) in the case of Cr(VI) and Cr(III) interacted bacterial cells, compared to the cells alone, can also be observed (Table 1). The shifts in binding energy for the aforementioned functional groups consequent to interaction with Cr(VI)/Cr(III) attests to the involvement of these functional groups either in the chemical interaction with chromium or in the donation of electrons to bring about the bioreduction of Cr(VI) to less toxic Cr(III).

3.2.3 *Electrokinetics Study*

It becomes of interest to examine the changes in the surface potential of the bacteria consequent to the interaction with chromium species. For this, zeta potential measurements were carried out for *C. paurometabolum* before and after interaction with varying concentrations of Cr(VI) as a function of pH. Figure 8a shows that the bacterial cells are negatively charged over a wide range of pH and the surface negative charge increases with increase in pH. Subsequent to interaction with Cr(VI) ions the zeta potential values for the bacteria are found to be less negative compared to the bacterial cells alone (Fig. 8a). It can also be observed from Fig. 8a that the magnitude of the decrease in the negative potential is found to increase with increase in Cr(VI) concentration (4–400 mg/L). The less negative surface charge obtained for the bacterial cells after interaction with Cr(VI) ions is due to the binding of positively charged Cr(III), formed as a result of bioreduction of Cr(VI) on the bacterial cell surface (Fig. 8a). It can also be noticed from Fig. 8a a marginal shift in the iso-electric point (IEP) of the bacterial cells from 2.5 to 3.2 subsequent to interaction with increasing concentration of Cr(VI) ions. The shift in IEP further confirms the involvement of chemical binding process in the interaction of Cr ions with the bacterial cell surface.

Apart from monitoring the changes in surface charge, concurrent analysis of chromium concentration on the bacterial cell surface and in the bulk solution was also carried out for the bacterial cells after interaction with chromium ions adopting the analytical techniques mentioned earlier. The total Cr uptake (mg/cell) and concentration of bioreduced Cr(III) in residual solution are depicted in Fig. 8b, c respectively, for the different conditions of experimentation. It is evident from Fig. 8b that the total Cr uptake increases with increase in Cr(VI) concentration and the maximum uptake is observed at pH 1 with the concentration sharply decreasing at alkaline pH values. The manifestation of the bioreduction of Cr(VI) to Cr(III) and the release of the latter to the solution is depicted in Fig. 8c. The bioreduction of Cr(VI) is found to increase with increase in its concentration. This substantiates the less negative surface potential values obtained for the bacterial cells interacted with higher concentrations of Cr(VI) (Fig. 8a).

The surface charge analysis of the bacterial cells was also carried out subsequent to interaction with Cr(III) ions as a function of pH. It can be observed that for the bacterial cells after biosorption of 4 mg/L of Cr(III), the zeta potential values become more positive vis-à-vis the cells alone especially in the pH range of 2–4 (Fig. 9a). This is due to the biosorption of the positively charged Cr(III) onto the bacterial surface. It can also be observed from Fig. 9a that at higher concentrations of Cr(III), the bacterial cells possess even more positive surface charges. Subsequent to the interaction of bacterial cells with 40 mg/L and 400 mg/L Cr(III) ions, the positive zeta potential values of bacterial cells show a maximum at pH 6 and beyond which the surface charge steeply decrease and become more negative in the pH range of 8–12 (Fig. 9a). It is noteworthy that the IEP of the bacterial cells is shifted from pH 2.5 to pH 4.5 after interaction with 4 mg/L Cr(III) and to pH 7–7.5 after interaction with 40–400 mg/L attesting to specific chemical interaction between Cr(III) and the bacteria.

The changes in the bacterial cell surface potentials could be attributed to the different Cr(III) species formed as a function of pH for the different concentrations studied.

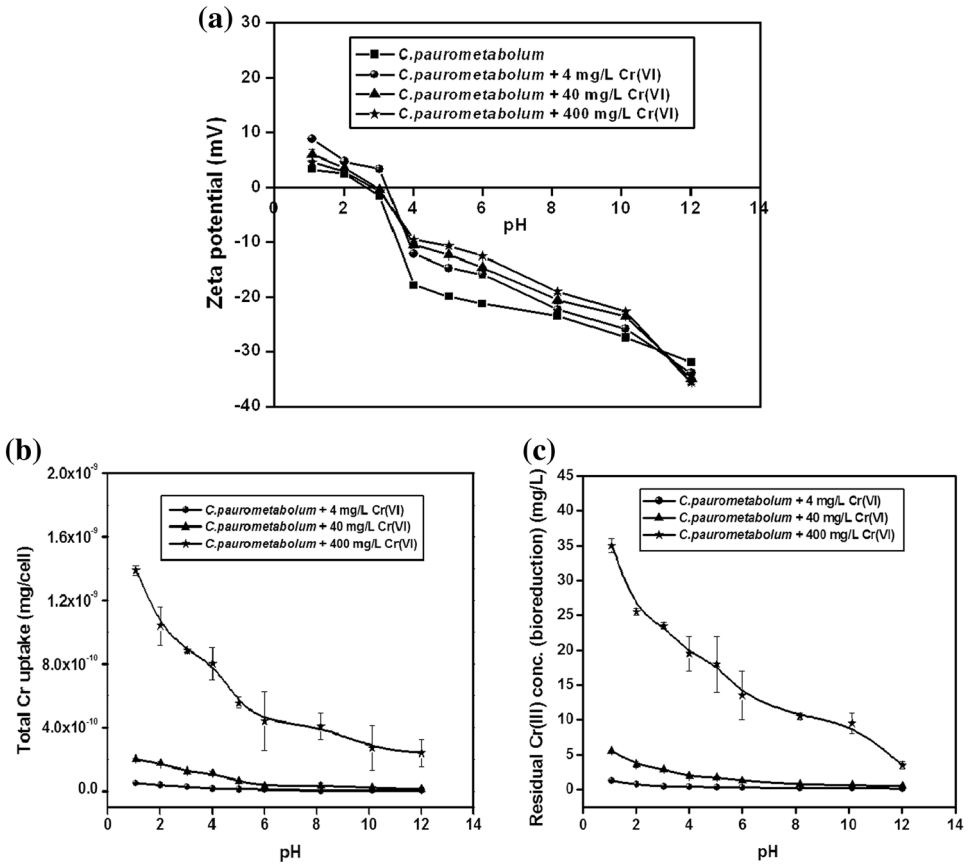

Fig. 8 **a** Zeta potential of *C. paurometabolum* before and after interaction with different concentrations of Cr(VI) as a function of pH, **b**, **c** Total Cr uptake (mg/cell) and residual bioreduced Cr(III) concentration obtained respectively on interaction of cells with different concentrations of Cr(VI) as a function of pH

Positively charged Cr^{3+} ions at acidic pH and positively charged hydroxyl species of Cr(III) such as $CrOH^{2+}$(aq) and $Cr(OH)_2^+$(aq) in the pH range of 4–10, contribute to make the surface charge of the bacterial cells less negative and even positive [34]. Cr(III) precipitates as $Cr(OH)_3$ species In the pH range of 5.5–12 onto the bacterial cell surface that influences the zeta potential values [26, 34]. In order to determine the role of the precipitated Cr(III) species at higher concentrations such as, 40 and 400 mg/L on the zeta potential values of the bacterial cells in the pH range of 5–9, independent experiments were carried out and the results are depicted in Fig. 9b. It can be observed from Fig. 9a, b, similarity between the zeta potential-pH relationship of the bacterial cells in the presence of 40 and 400 mg/L Cr(III) concentrations with a maxima at around pH 6 and the zeta potential trend as a function of pH for the precipitated Cr(III) species at the two concentrations studied (Fig. 9a, b). Thus, the surface charge of the bacterial cells at higher concentration of Cr(III) are dictated by the surface active precipitates of Cr(III) species.

Additionally, Cr(III) concentration in the bulk solution in the absence and presence of the bacterial cells as a function of pH was monitored (Fig. 9c–e). From Fig. 9c it can be observed that in the absence of the bacterial cells, Cr(III) of 4 mg/L concentration is relatively stable up to pH 3 and is almost completely precipitated in the pH range of 8–10 and the precipitate is resolubilised to $Cr(OH)_4^-$ species beyond pH 10. The different Cr(III) species formed as a function of pH are in agreement with the earlier findings [32]. However, in the presence of bacterial cells, Cr(III) residual concentration steadily decreases with increase in pH from 1 to 6 attributable to increase in Cr(III) uptake by the cells as a function of pH and beyond pH 6 Cr(III) uptake is found to decrease due to the electrostatic repulsion between negatively charged bacterial cell surface and anionic hydroxyl species of Cr(III) ($Cr(OH)_4^-$) (Fig. 9c). The residual Cr(III) concentration for bacterial cells subsequent to interaction with higher concentrations (40 and 400 mg/L) of Cr(III) as a function of pH are depicted in Fig. 9d, e respectively. In the absence of the bacterial cells the decrease in Cr(III) concentration follows similar trends to that observed for 4 mg/L concentration of Cr(III) (Fig. 9d, e). In the case of 40 mg/L Cr(III) concentration, in the absence of bacterial cells, complete precipitation of Cr(III) species is observed in the pH range of 8–12 (Fig. 9d). However, in the presence of bacterial cells at 40 mg/L Cr(III) concentration, significant precipitation of Cr(III) species can be observed in the pH range of 6–10 and resolubilisation to $Cr(OH)^{4-}$ takes place beyond that pH (Fig. 9d). At 400 mg/L Cr(III) concentration, complete

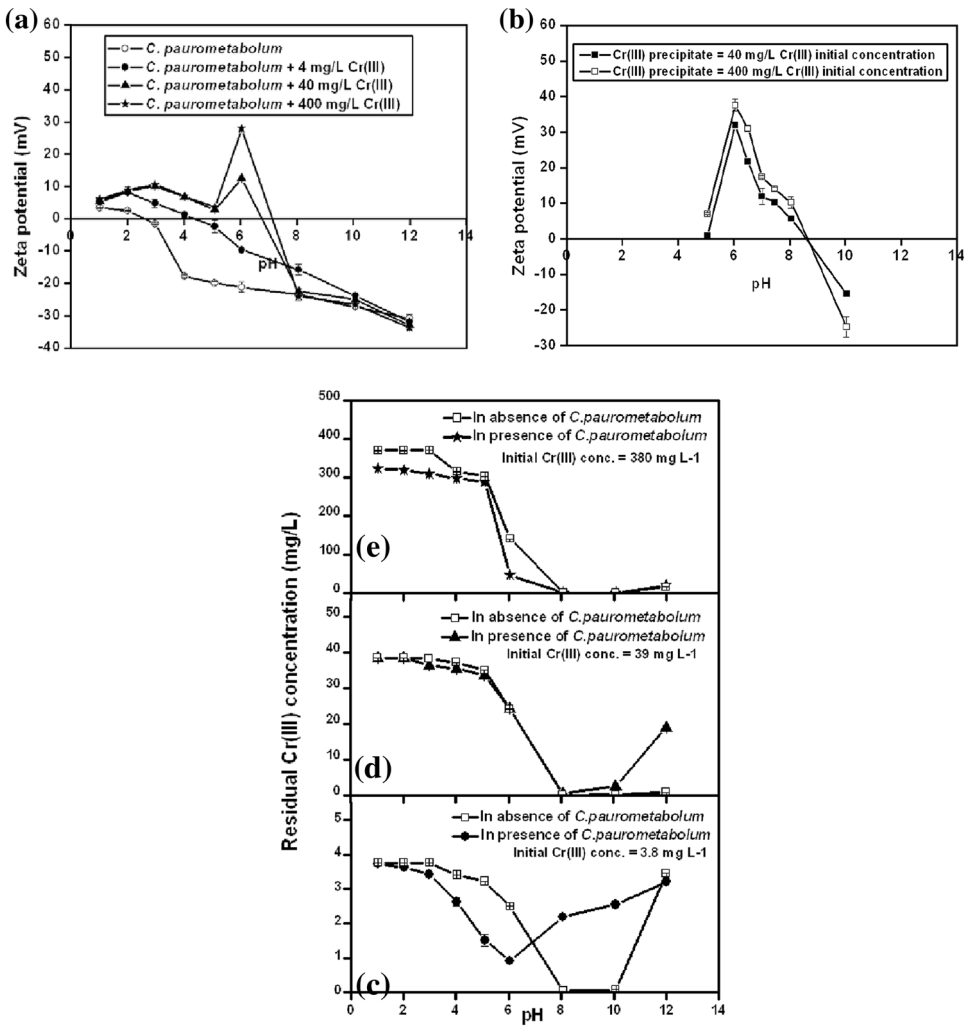

Fig. 9 **a** Zeta potential of *C. paurometabolum* before and after interaction with different concentrations of Cr(III) as a function of pH, **b** Zeta potential of Cr(III) precipitate as a function of pH for initial Cr(III) concentrations of 40 and 400 mg/L; **c–e** Residual concentration of Cr(III) as a function of pH before and after interaction with *C. paurometabolum* for 4, 40 and 400 mg/L Cr(III) concentrations, respectively

precipitation of Cr(III) species is observed in the pH range of 8–12 both in the absence and presence of bacterial cells (Fig. 9e).

3.2.4 *Mechanisms of Bioremediation Involved at the C. paurometabolum-Chromium Solution Interface*

In the light of the experimental results obtained for the biosorption and characterisation studies, the bioremediation of chromium by *C. paurometabolum* has been schematically represented in Fig. 10. It may be recalled that the biosorption isotherms of *C. paurometabolum* for Cr(VI) and Cr(III) are found to exhibit a typical Langmuirian behaviour and the free energy values are indicative of a chemisorption process. ATR-FTIR studies reveal shifts in the wavenumbers of characteristic functional groups such as –OH, –COOH, –NH and those containing phosphorus, corroborating to their involvement in the complexation with the chromium species. X-ray photoelectron spectroscopic data confirms the binding of the bioreduced Cr(III) onto the bacterial cell surface. The occurrence of the bioreduction process is further substantiated from the zeta potential measurements carried out for the bacterial cells subsequent to interaction with chromium ions. Additionally, the shifts in the iso-electric point of the bacterial cells after interaction with chromium species, confirm the involvement of chemical binding forces between the binding groups present on the bacterial cell surface and chromium. The cell wall of *C. paurometabolum* (acid fast Gram positive bacterium) is composed of two major components, namely, peptidoglycan layer followed by a glycolipid layer composed of arabinogalactose, lipoarabinomannan, mycolic acids and surface proteins [35]. Moreover, the cell wall of Gram positive bacterial cell exposes numerous teichoic acids that are polyol phosphate polymers with either ribitol or glycerol linked by phosphodiester bond [36]. Thus, the cell wall components of the bacterial cells are composed of a myriad of functional groups that expose sites for the binding of chromium ions. From Fig. 10, it can be seen that all the

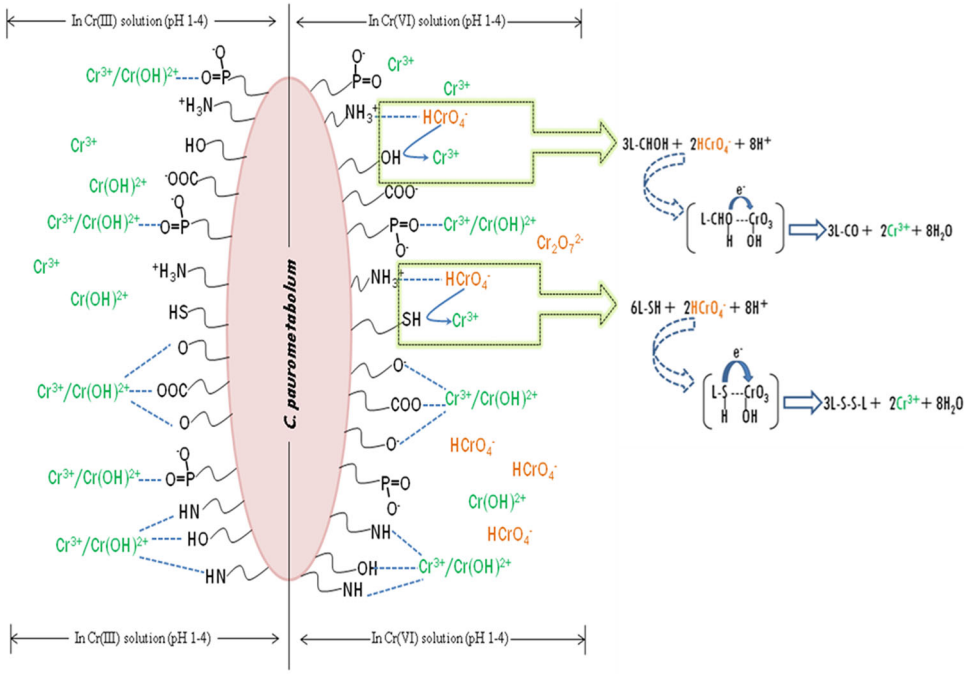

Fig. 10 Schematic diagram of the mechanisms involved in biosorption and bioreduction of Cr(VI); and biosorption of Cr(III) using *C. paurometabolum*

amino groups exposed by the *C. paurometabolum* bacterial cell surface in the pH range 1–4 are protonated. The binding of the negatively charged oxyanions of Cr(VI) ions onto the protonated sites present on the bacterial cell surface occurs via electrostatic interactions. It can be observed from Fig. 10 that, consequent to the binding of Cr(VI) ions, adjacent ligands (L)/cell wall components composed of functional groups such as –OH and –SH that are electron donors, bring about the reduction of Cr(VI) to Cr(III) ions. Prior to the bioreduction process, Cr(VI) oxyanions form chromate ester intermediates with the hydroxyl and sulphydryl groups present on the bacterial cell surface. The chromate ester intermediates thus formed, decompose immediately, with concurrent transfer of electrons from oxygen of chromate oxyester or from sulphur of chromate thioester to the electron accepting Cr(VI) center, thereby resulting in the bioreduction of Cr(VI) to Cr(III) ions (Fig. 10). From Fig. 10, it can also be observed that the Cr(III) ions formed via the bioreduction of Cr(VI) are either released to the bulk solution or form chemical complexes with the functional groups such as hydroxyl, carboxyl, amino and phosphorus containing groups present on the bacterial cell surface. Thus, bioremediation of Cr(VI) by the bacterial cells is governed by two processes, namely, biosorption of chromium, that involves both electrostatic and chemical interactions and bioreduction of Cr(VI) to the less toxic Cr(III). On the other hand, bioremediation of Cr(III) by the bacterial cell as represented in Fig. 10 is achieved by the formation of chemical complexes with hydroxyl, carboxyl, amino and phosphorus containing functional groups present on the bacterial cell surface.

4 Conclusions

Based on the bioremediation studies of Cr(VI) and Cr(III) ions carried out using a Gram positive acid fast bacterium, *C. paurometabolum*, as a biosorbent, the following conclusions can be drawn:

- The bioremediation studies of Cr(VI) using *C. paurometabolum* resulted in about 50% biosorption at an equilibrium time of 2 h, initial Cr(VI) concentration of 4 mg/L, pH 1 and a biomass loading of 3.1×10^{10} - cells/mL.
- The remainder, 50% was found to be in the form of less toxic Cr(III) ions owing to bioreduction of Cr(VI) by the bacterial cells, that resulted in a nil concentration of Cr(VI) ions in the residue, thereby meeting the USEPA specifications for safe effluent discharge.
- Studies on bioremediation of Cr(III) solution using *C. paurometabolum* resulted in a maximum biosorption of 55% at an equilibrium time of 2 h, Cr(III) concentration of 4 mg/L, pH 3 and a biomass loading of 3.4×10^{10} cells/mL.
- The bioremediation of Cr(VI) by the bacterial cells is found to follow pseudo first order kinetics while pseudo second order kinetic is followed during the Cr(III) biosorption process.

- The biosorption isotherms of Cr(VI) and Cr(III) were found to follow a typical Langmuirian behaviour.
- The Gibbs free energies (ΔG) were determined to be -25.5 and -29.5 kJ/mol respectively for Cr(VI) and Cr(III), suggestive of chemisorption between the binding groups present on bacterial cell surface and chromium ions.
- The desorption of Cr(VI) or Cr(III) from the bacterial cells, initially interacted with the chromium species indicated only a marginal release into the bulk solution, attesting to the irreversible nature of biosorption.
- FTIR studies revealed the involvement of hydroxyl, carboxyl, amino and phosphate groups in the biosorption of Cr(VI) and Cr(III).
- Electrokinetic and X-ray photoelectron spectroscopic studies provided further evidence in support of biosorption and bioreduction mechanisms of chromium remediation.
- The mechanisms of bioremediation of Cr(VI) by *C. paurometabolum* can be thus be unequivocally stated to be involving both biosorption and bioreduction processes, as compared to only biosorption in the case of studies related to bioremediation of Cr(III).

Acknowledgements The authors are grateful to the Institute of Research for Development (IRD), France for sponsoring a research project. DCP thanks the Ministry of Human Resource Development (MHRD), Government of India for grant of a research fellowship.

References

1. Gad S C, *Sci Total Environ* **86** (1989) 149.
2. Das A P, and Mishra S, *J Carcinog* **9** (2010) 1.
3. Amiri M J, Fadaei E, Baghvand A, and Ezadkhasty Z, *Int J Environ Res* **8** (2014) 411.
4. Levis A G, and Bianchi V, in *Biological and Environmental Aspects of Chromium*, (ed) Langard S, Elsevier Biomedical Press, New York (1982), p 171.
5. Barnhart J, *J Soil Contam* **6** (1997) 561.
6. Kimbrough D E, Cohen Y, Winer A M, Creelman L and Mabuni C, *Crit Rev Environ Sci Technol* **29** (1999) 1.
7. Hawley E L, Deeb R A, Kavanaugh M C, and Jacobs J R G, in *Chromium(VI) Handbook*, (eds) Guertin J, Avakian C P, and Jacobs J A, CRC Press, Boca Raton (2004), p 273.
8. Agrawal A, Kumar V, and Pandey B D, *Process Extr Metall Rev* **27** (2006) 99.
9. Owlad M, Aroua M K, Daud W A W, and Baroutian S, *Water Air Soil Pollut* **200** (2009), 59.
10. Oliveira R C, Palmieri C, and Garcia O, in *Progress in Biomass and Bioenergy Production*, (ed) Shaukat S S, In Tech, Croatia (2011), p 151.
11. Sen R, and Chakrabarti S, *Curr Sci* **97** (2009) 768.
12. Volesky B, *Sorption and biosorption*, BV Sorbex Inc, Canada (2003).
13. Gupta R, Ahuja P, Khan S, Saxena R K, and Mohapatra H, *Curr Sci* **78** (2000) 967.
14. Gadd G M, *J Chem Technol Biotechnol* **84 (**2009) 13.
15. Park D, Yun Y-S, and. Park J M, *Biotechnol Bioprocess Eng* **15** (2010) 86.
16. Atkinson B W, Bux F, and Kasan H C, *Water SA* **24** (1998) 129.
17. Mohan D, and Pittman C U, *J Hazard Mater* **B137** (2006) 762.
18. Vijayaraghavan K, and Yun Y-S, *Biotechnol Adv* **26** (2008) 266.
19. Sen M, and Dastidar M G, *Iran J Environ Health Sci Eng* **7** (2010) 182.
20. Ray S A, and Ray M K, *Al Ameen J Med Sci* **2** (2009) 57.
21. Saha B, and Orvig C, *Coord Chem Rev* **254** (2010) 2959.
22. Paul M L, Samuel J, Chandrasekaran N, and Mukherjee A, *Chem Eng J* **187** (2012) 104.
23. Silva B, Figueiredo H, Quintelas C, Neves I C, and Tavares T, *Int Biodeter Biodegr* **74** (2012) 116.
24. Rai D, Eary L E, and Zachara J M, *Sci Total Environ* **86** (1989) 15.
25. Ball J W, and Nordstrom D K, *J Chem Eng Data* **43** (1998) 895.
26. Kotaś J, and Stasicka Z, *Environ Pollut* **107** (2000) 263.
27. Sekhar K C, Subramanian S, Modak J M, and Natarajan K A, *Int J Miner Process* **53** (1998) 107.
28. Giles C H, MacEvan T H, Nakhwa S N, and Smith D, *J Chem Soc* (1960) 3973.
29. Langmuir I, *J Am Chem Soc* **40** (1918) 1361.
30. Socrates G, *Infrared and Raman characteristic group frequencies: tables and charts*, Wiley, Chichester (2004), p 50.
31. Jiang W, Saxena A, Song B, Ward B B, Beveridge T J, and Myneni S C B, *Langmuir* **20** (2004) 11433.
32. Dambies L, Guimon C, Yiacoumi S, and Guibal E, *Colloids Surf A* **177** (2001) 203.
33. Park D, Lim S-R, Yun Y-S, and Park, J M, *Chemosphere* **70** (2007) 298.
34. Rai D, Sass B M, and Moore D A, *Inorg Chem* **26** (1987) 345.
35. Lederer E, *Pure Appl Chem* **25** (1971) 135.
36. Willey J M., Sherwood L M, and Woolverton C J, *Prescott, Harley and Klein's Microbiology*, McGraw-Hill Companies Inc., New York (2008), p 57.